

Interplay of Linker, *N*-Substituent, and Counterion Effects in the Formation and Geometrical Distortion of *N*-Heterocyclic Biscarbene Complexes of Rhodium(I)

Chin Hin Leung, Christopher D. Incarvito, and Robert H. Crabtree*

Department of Chemistry, 225 Prospect Street, Yale University, New Haven, Connecticut 06520-8107

Received August 8, 2006

A new series of (CH₂)_{*n*}-linked *N*-heterocyclic biscarbene (bis-NHC) complexes of rhodium(I) have been synthesized via in situ generation of the silver carbene complexes from bis(imidazolium) halide salts and silver(I) oxide followed by transmetalation to [Rh(COD)Cl]₂ (COD = 1,5-cyclooctadiene). With a large *t*-Bu *N*-substituent, short linkers favor the chelate and long linkers favor the 2:1 complex, contrary to the previous findings with the small *n*-Bu substituent. In addition, the use of a noncoordinating anion for the AgNHC favors chelate formation. The chelate complex [Rh(COD)L₂]PF₆ (L₂ = [methylenebis(*N*-(*tert*-butyl)imidazol-2-ylidene)]) and its dicarbonyl analogue [Rh(CO)₂L₂]PF₆ were structurally characterized. They showed distortion both of the square plane, an electronic effect, and of the metal–NHC moiety, a steric effect.

Introduction

The importance of chelating versions of other common ligand classes means that chelating *N*-heterocyclic carbenes (NHCs)¹ are likely to be increasingly useful in organometallic synthesis and catalysis. Differing from their bis-phosphine analogues, however, the general principles governing the use of chelating NHCs have yet to be established, and it is already clear that numerous potential complications can arise.² Unlike the phosphine ligand, which has a cone shape, the NHC ligand is fan-shaped with the *N*-substituents inclining toward the metal center. In addition, the metal–NHC bond is in general less labile than metal–phosphine bonds, but the cleavage of the MC bond to give the imidazolium salt, when it does occur, is often irreversible.³

In a previous study, we have observed that the precursor bis(imidazolium) salts **1**^{*n*-Bu} can successfully coordinate to a Rh(I) center in either a chelating or a bridging 2:1 fashion (Scheme 1), depending on the length of the linker between the two NHCs.^{2b} This behavior was rationalized on the basis that the NHC plane prefers on steric grounds to lie in the ±*z* direction (out of the *xy* square coordination plane). In the chelate, this can be achieved only with a long linker (*n* = 3 or 4). With a

short linker (*n* = 1 or 2) theazole rings would be forced to adopt a chelate conformation in which theazole ring planes are significantly displaced from the optimal ±*z* direction. The steric clash of the *N*-substituents of the NHC with the COD groups that would result in the chelate was proposed to cause the system to prefer the 2:1 structure **3**, where both NHCs can adopt a strictly ±*z* conformation.

In this prior work^{2b} on bis-NHC chelates, the sterically small *n*-butyl group was always the substituent at nitrogen; it was plausibly assumed that this small group played little role in the chemistry. In catalytic applications, however, bulky groups are much more commonly employed. Results by others⁴ have also suggested that, apart from linker length, the steric size of the *N*-substituents as well as choice of counterion for the AgNHC intermediate can affect the coordination mode of bis-NHCs. In this current study we report the synthesis of a series of bis-NHC compounds of Rh(I). We find significant effects on product geometry and stoichiometry using bulkier *t*-Bu groups as *N*-substituents instead of *n*-Bu and also using noncoordinating anions in the AgNHC. Two of the resulting Rh(I) chelate complexes were structurally characterized and show two types of distortions. The first involves bending of the square plane and is predominantly electronic in origin. The second, an unusual “yaw” distortion of the M–NHC system, involves rotation of the NHC about the axis normal to theazole plane and has a steric origin.

Results

Synthesis of Ligand Precursors. Bis(imidazolium) dibromide salts with *t*-Bu (**1c-d**^{*t*-Bu}) or *i*-Pr *N*-substituents (**1c**^{*i*-Pr}) were synthesized by the reaction of 1-alkylimidazole and the corresponding dibromoalkanes.⁵ The product identities were confirmed by ¹H and ¹³C NMR, electrospray ionization MS (ESI-MS), and elemental analysis. In particular the C2 protons of the imidazole rings display a characteristic downfield

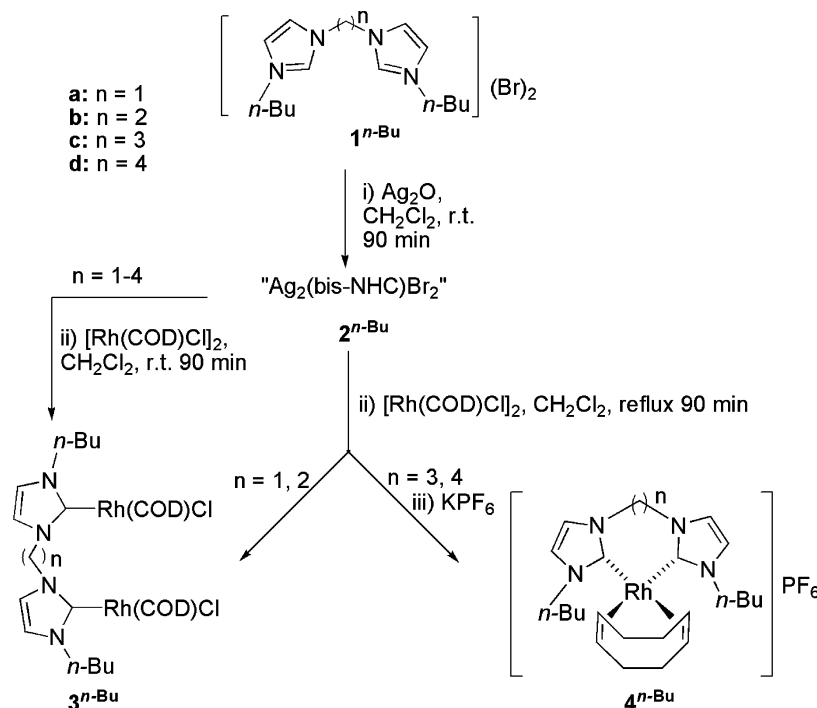
* Corresponding author. E-mail: robert.crabtree@yale.edu.

(1) For recent reviews, see: (a) Mata, J. A.; Poyatos, M.; Peris, E. *Coord. Chem. Rev.* **2006**, doi:10.1016/j.ccr.2006.06.008. (b) Scott, N. M.; Nolan, S. P. *Eur. J. Inorg. Chem.* **2005**, 1815–1828. (c) Cavallo, L.; Correa, A.; Costabile, C.; Jacobsen, H. *J. Organomet. Chem.* **2005**, 690, 5407–5413. (d) Cavell, K. J.; McGuinness, D. S. *Coord. Chem. Rev.* **2004**, 248, 671–681. (e) Peris, E.; Crabtree, R. H. *Coord. Chem. Rev.* **2004**, 248, 2239–2246. (f) Herrmann, W. A. *Angew. Chem., Int. Ed.* **2002**, 41, 1291–1329. (g) Bourissou, D.; Guerret, O.; Gabbai, F. P.; Bertrand, G. *Chem. Rev.* **2000**, 100, 39–91.

(2) (a) Appelhans, L. N.; Zuccaccia, D.; Kovacevic, A.; Chianese, A. R.; Miecznikowski, J. R.; Macchioni, A.; Clot, E.; Eisenstein, O.; Crabtree, R. H. *J. Am. Chem. Soc.* **2005**, 127, 16299–16311, and reference therein. (b) Mata, J. A.; Chianese, A. R.; Miecznikowski, J. R.; Poyatos, M.; Peris, E.; Faller, J. W.; Crabtree, R. H. *Organometallics* **2004**, 23, 1253–1263. (c) Herrmann, W. A.; Kocher, C.; Goossen, L. J.; Artus, G. R. *J. Chem. Eur. J.* **1996**, 2, 1627–1636.

(3) (a) Crudden, C. M.; Allen, D. P. *Coord. Chem. Rev.* **2004**, 248, 2247–2273. (b) McGuinness, D. S.; Cavell, K. J.; Skelton, B. W.; White, A. H. *Organometallics* **1999**, 18, 1596–1605.

(4) (a) Wanniarachchi, Y. A.; Khan, M. A.; Slaughter, L. M. *Organometallics* **2004**, 23, 5881–5884. (b) Burling, S.; Field, L. D.; Li, H. L.; Messerle, B. A.; Turner, P. *Eur. J. Inorg. Chem.* **2003**, 3179–3184.

Scheme 1. Linker Dependence in the Formation of 2:1 and Chelate Bis-NHC Complexes of Rh(I) from the Precursors $1^{n\text{-Bu}}$,^{2b}

resonance at ~ 10 ppm, characteristic of an imidazolium salt. Interestingly, we found that the known ethylene bis(*N*-(*tert*-butyl)imidazolium bromide)^{5c} decomposes in methanol, probably through Hoffman elimination of the β -hydrogen to form the 1-(*tert*-butyl)-3-vinyl imidazolium bromide, as evidenced by the presence of an ESI-MS peak for the cation at 151.

Transmetalation from Silver NHC Complexes with a Halide Counterion. Following the conditions of Lin,⁶ the silver carbene complexes **2** were generated in situ by reaction of Ag_2O with the bis(imidazolium) bromide salts in CH_2Cl_2 at room temperature. The mild silver transmetalation method is the preferred way to generate $(\text{CH}_2)_n$ -linked bis-NHCs because C–H bonds of the alkyl linkers α (and β) to the imidazole nitrogen could provide alternative deprotonation pathways if harsher conditions were used. Generation of silver carbene is accompanied by loss of the C2 proton NMR signal of the imidazole at ~ 10 ppm accompanied by an upfield shift of the C4 and C5 protons to ~ 7 ppm.⁷ After removal of insoluble solids, the filtrate was combined with 0.5 equiv of $[\text{Rh}(\text{COD})\text{Cl}]_2$ (Rh:bis-NHC precursor, 1:1) in refluxing CH_2Cl_2 . Immediate generation of silver halide as a white precipitate was observed, and the reaction mixtures were left for another 45 min before workup (Scheme 2).

For the $n = 1$ case, even though green decomposition products appeared within 30 min, the unstable chelate product $4^{t\text{-Bu}}$ could still be isolated. Column chromatography yields the PF_6^-

analogue (eluent: acetone/ KPF_6) in very low yield. No neutral 2:1 species were observed. The ^1H NMR spectrum of the chelate complex is characterized by two broad peaks at 4.5 ppm corresponding to the COD vinyl protons and an AB pattern centered at 6.5 ppm ($^2J_{\text{H-H}} = 13.0$ Hz) for the bridging methylene protons, consistent with the usual^{4,8} nonfluxional puckered structure with a plane of symmetry bisecting the bis-NHCs and the COD. The carbene carbon signal appears at 180.4 ppm and showed Rh–C coupling of 51.8 Hz.

For the $n = 2$ – 4 cases, 2:1 complexes formed and were isolated by column chromatography in low yields (10–15% based on Rh). Oxidation by excess Ag(I) species could be one source of these low yields,⁹ although we were unable to isolate any Rh(III) species. At a Rh to bis-NHC precursor ratio of 2:1 instead of 1:1, the yields were significantly improved (40–62% based on Rh). The ^1H NMR spectra are characterized by four broad signals (3–5 ppm), corresponding to the four nonequivalent vinyl protons of the COD groups in the 2:1 species. The ^{13}C NMR spectra showed the Rh-bound carbene carbons in the expected range of 179.1–180.5 ppm ($J_{\text{Rh-C}} = 49.8$ – 51.4 Hz). As in the previous *n*-Bu case,^{2b} two diastereomers (*dl* and *meso*) are present, due to the restricted rotation about the M–carbene bond. The decreasing diastereoselectivity of the *t*-Bu complexes (*dl*:*meso* ratios: $n = 2$, 100:0; $n = 3$, 60:40; $n = 4$, 50:50) with increasing linker length is also similar to that found for the *n*-Bu case ($n = 2$, 95:5; $n = 3$, 60:40; $n = 4$, 50:50) and is ascribed to decreasing steric interactions between the metal centers as the linker length, n , increases.

On the hypothesis that there is a steric clash between the *t*-Bu groups that disfavors the formation of chelate analogues of $4^{t\text{-Bu}}$ with a long linker (e.g., $n = 3$), we moved to an *i*-Pr substituent because models suggested such a clash could then be avoided. Under otherwise identical conditions, changing the

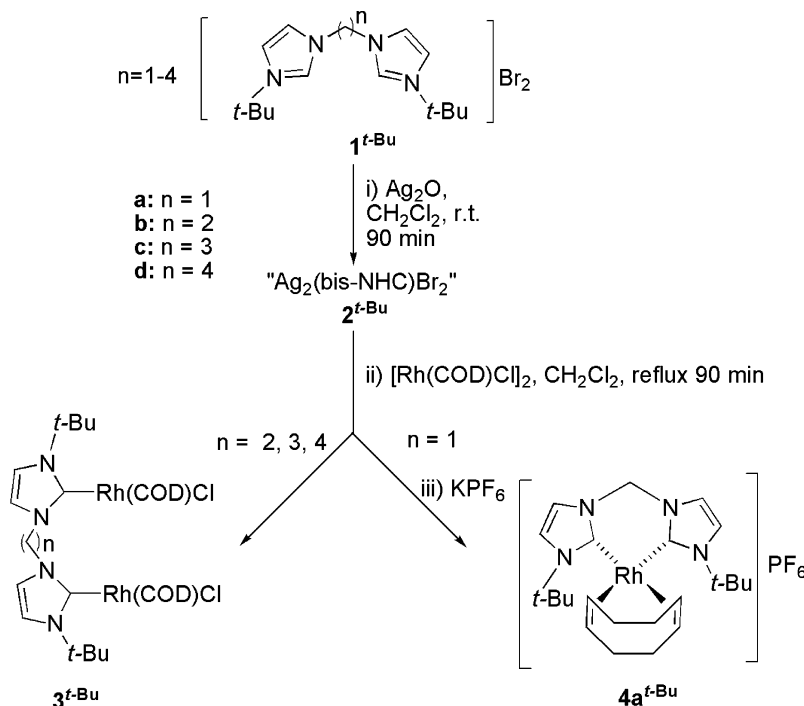
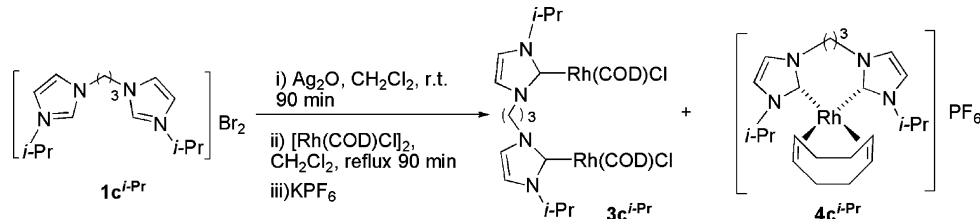
(5) (a) Albrecht, M.; Miecznikowski, J. R.; Samuel, A.; Faller, J. W.; Crabtree, R. H. *Organometallics* **2002**, *21*, 3596–3604. (b) Herrmann, W. A.; Schwarz, J.; Gardiner, M. G. *Organometallics* **1999**, *18*, 4082–4089. (c) Douthwaite, R. E.; Haussinger, D.; Green, M. L. H.; Silcock, P. J.; Gomes, P. T.; Martins, A. M.; Danopoulos, A. A. *Organometallics* **1999**, *18*, 4584–4590.

(6) (a) Lin, I. J. B.; Vasam, C. S. *Comments Inorg. Chem.* **2004**, *25*, 75–129. (b) Chianese, A. R.; Li, X.; Janzen, M. C.; Faller, J. W.; Crabtree, R. H. *Organometallics* **2003**, *22*, 1663–1667. (c) Wang, H. M. J.; Lin, I. J. B. *Organometallics* **1998**, *17*, 972–975.

(7) (a) Chiu, P. L.; Chen, C. Y.; Zeng, J. Y.; Lu, C. Y.; Lee, H. M. J. *Organomet. Chem.* **2005**, *690*, 1682–1687. (b) Quezada, C. A.; Garrison, J. C.; Panzner, M. J.; Tessier, C. A.; Youngs, W. J. *Organometallics* **2004**, *23*, 4846–4848.

(8) Bertrand, G.; Diez-Barra, E.; Fernandez-Baeza, J.; Gornitzka, H.; Moreno, A.; Otero, A.; Rodriguez-Curiel, R. I.; Tejada, J. *Eur. J. Inorg. Chem.* **1999**, 1965–1971.

(9) Mas-Marza, E.; Poyatos, M.; Sanau, M.; Peris, E. *Inorg. Chem.* **2004**, *43*, 2213–2219.

Scheme 2. Formation of 2:1 or Chelate Bis-NHC Complexes of Rh(I) from the Precursors $1^{t\text{-Bu}}$.Scheme 3. Formation of Both 2:1 ($3c^{i\text{-Pr}}$) and Chelate ($4c^{i\text{-Pr}}$) Complexes (7:4 molar ratio) from Precursor $1c^{i\text{-Pr}}$ 

wingtip group of the trimethylene-linked precursor from *t*-Bu to *i*-Pr indeed results in a 4:7 ratio of chelate versus dimetallic 2:1 products (Scheme 3). The two products could be separated by column chromatography. The ^1H NMR of the 2:1 complex $3c^{i\text{-Pr}}$ showed the expected four broad signals for the four inequivalent COD vinyl groups and of two diastereomeric sets of CH_3 signals for the *i*-Pr groups. The C(carbene) signal appears at 180 and 181 ppm (as in $3^{t\text{-Bu}}$, two diastereomers are present), and both showed Rh–C coupling of 51 Hz. Consistent with a chelate structure, complex $4c^{i\text{-Pr}}$ showed two broad ^1H NMR signals for the COD vinyl protons. The C(carbene) signal appears at 180.9 ppm ($^1J_{\text{Rh-C}}$: 54.4 Hz).

Transmetalation with a Noncoordinating Counterion. As noncoordinating anions have been found to favor chelation over production of 2:1 complexes,⁴ Ag(I)–NHC transmetalation agents with PF_6^- counterion, " $\{\text{Ag}_2(\text{bis-NHC})\}(\text{PF}_6)_2$ ",¹⁰ were formed and directly used for transmetalation to $[\text{Rh}(\text{COD})\text{Cl}]_2$. In a modification of a previously published method,^{7b} " $\text{Ag}_2(\text{bis-NHC})\text{Br}_2$ " were generated by reaction of the bis(imidazolium) salts and Ag_2O in water. Addition of excess KPF_6 yields the PF_6^- analogues as white precipitates, which, after drying in vacuo, were immediately used for transmetalation to $[\text{Rh}(\text{COD})\text{Cl}]_2$ in CH_2Cl_2 . Under the same conditions in which the original " $\text{Ag}_2(\text{bis-NHC})\text{Br}_2$ " reagent failed to lead to chelate formation, the PF_6^- salts gave the novel chelate complexes $4a^{n\text{-Bu}}$ and $4b^{t\text{-Bu}}$ (Scheme 4). We have been unable to determine if $4a^{n\text{-Bu}}$

and $4b^{t\text{-Bu}}$ are thermodynamic or kinetic products, so thermodynamic arguments may not be appropriate here.

Compound $4a^{n\text{-Bu}}$ has a ^1H NMR spectrum similar to that of $4a^{t\text{-Bu}}$. Apart from the characteristic AB pattern and the two broad signals of the COD vinyl protons, the wingtip *n*-Bu signals appear as a set of diastereotopic pairs, as in the previously reported $n=2-4$ analogues.^{2b} In solution, $4a^{n\text{-Bu}}$ decomposes within minutes, however, going from its original orange color to a green NMR-silent species.

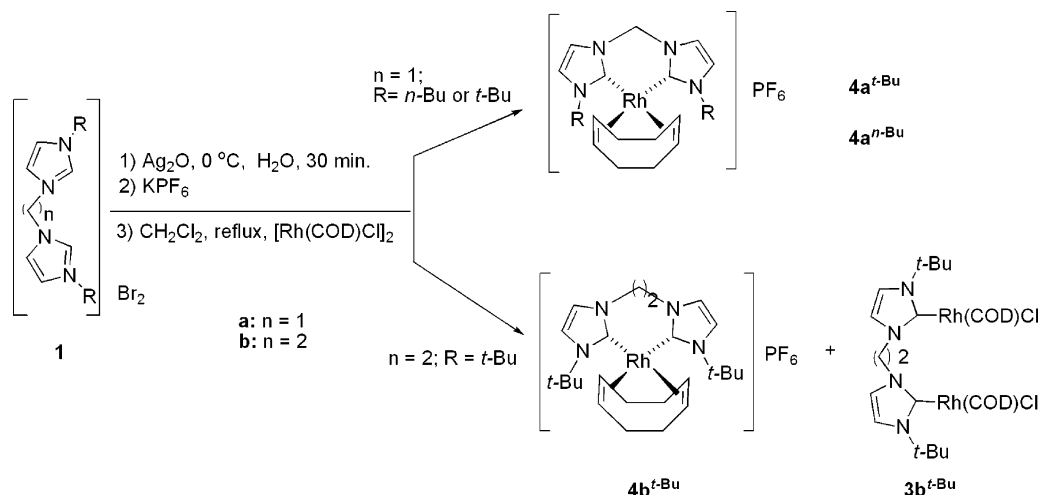
Ethylene linkers seem to be unstable in this system. Under identical conditions, the ethylene-linked precursor $1b^{t\text{-Bu}}$ gave both the neutral $3b^{t\text{-Bu}}$ and a cationic species that we could not isolate but is likely to be $4b^{t\text{-Bu}}$, as suggested by ^1H NMR and ESI-MS.¹¹ Although Hoffmann elimination in the precursor $1b^{t\text{-Bu}}$ has been observed in the ESI-MS, we did not observe the vinyl species either free or coordinated in samples of $4b^{t\text{-Bu}}$.

The PF_6^- salt of $4a^{t\text{-Bu}}$ was also synthesized directly in somewhat higher yield (29%) using this method, avoiding the unstable halide species. Unlike $4a^{n\text{-Bu}}$, $4a^{t\text{-Bu}}$ is stable in CH_2Cl_2 for days under air. The dicarbonyl analogue $[\text{Rh}(\text{CO})_2\text{L}_2]\text{PF}_6$ $5a^{t\text{-Bu}}$ formed readily when carbon monoxide was passed through a solution of $4a^{t\text{-Bu}}$ (1 atm, CH_2Cl_2 , 20 min). In the ^{13}C NMR spectrum the carbonyl carbon signal appears at 187.5 ppm ($^1J_{\text{C-Rh}} = 59.3$ Hz), and the carbene carbons appear at 171.4 ppm ($^1J_{\text{C-Rh}} = 49.4$ Hz).

X-ray Crystallography. Crystals of both $4a^{t\text{-Bu}}$ and $5a^{t\text{-Bu}}$ suitable for X-ray diffraction analysis were crystallized from

(10) Stoichiometry is based on analogous silver carbene complexes that have been structurally characterized. See Refs 4a and 7.

(11) For spectral details, see Supporting Information.

Scheme 4. Generation of Bis-NHC Rh(I) Complexes by Transmetalation with Hexafluorophosphate as Anion^a

^a For $n = 2$, a 1:1 ratio of **4b^{t-Bu}** and **3b^{t-Bu}** was formed based on ¹H NMR.

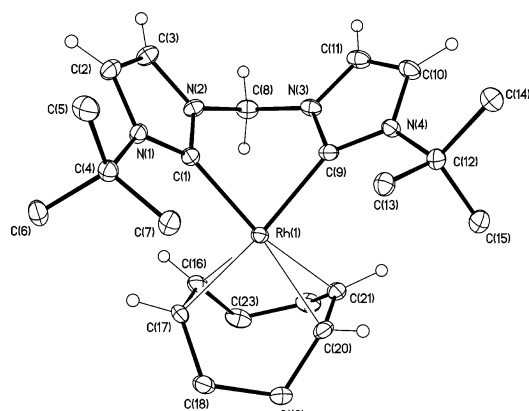


Figure 1. ORTEP diagram of **4a^{t-Bu}**, showing 30% ellipsoids. The counterion and the *t*-Bu and COD allyl hydrogens are omitted for clarity.

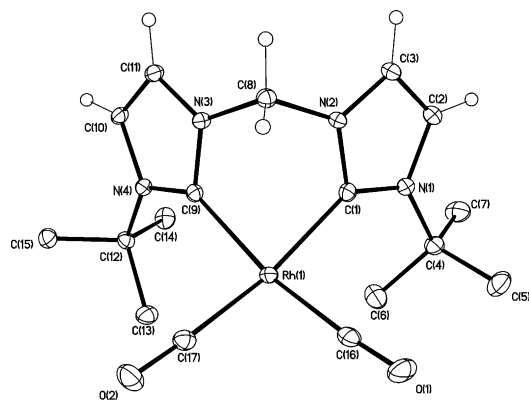


Figure 2. ORTEP diagram of **5a^{t-Bu}**, showing 30% ellipsoids. The counterion and hydrogen atoms on the *t*-Bu groups are omitted for clarity.

CH₂Cl₂/pentane, and the results (Figures 1 and 2) confirmed the proposed chelate structures. As in other methylene-linked square planar bis-NHC complexes,¹² the metallacycle ring assumes the expected puckered form. Selected bond lengths and angles are listed in Table 1. The Rh–C(carbene) bond lengths (2.036–2.092 Å) are comparable to those of analogous Rh bis-NHC chelates^{2b,4} and longer than the average Rh–C(carbene) distance for monodentate NHCs (1.97 Å).¹³ The C(carbene)–Rh–C(carbene) bite angle is 81.5° for both structures, probably reflecting the constraint of the six-membered metallacycle.

Table 1. Selected Bond Distances in **4a^{t-Bu}** and **5a^{t-Bu}**

	4a^{t-Bu} [Rh(COD)(bis-NHC)] ⁺	5a^{t-Bu} [(CO) ₂ Rh(bis-NHC)] ⁺
Rh–C (carbene)		
Rh(1)–C(1)	2.036(3)	2.077(2)
Rh(1)–C(9)	2.092(3)	2.078(2)
Rh–C (COD or diCO)		
Rh(1)–C(16)	2.156(3)	1.895(3)
Rh(1)–C(17)	2.193(3)	1.905(3)
Rh(1)–C(20)	2.206(3)	
Rh(1)–C(21)	2.207(3)	
C–O		
O(1)–C(16)		1.130(3)
O(2)–C(17)		1.124(3)
Bite Angle (C–Rh–C)		
C(1)–Rh(1)–C(9)	81.53(12)	81.49(9)
C(16)–Rh(1)–C(17)		91.71(11)
(dicarbonyl)		
N–C(carbene)–Rh		
N(1)–C(1)–Rh(1)	138.8(2)	139.79(17)
N(2)–C(1)–Rh(1)	116.4(2)	115.29(15)
N(4)–C(9)–Rh(1)	142.4(2)	140.18(16)
N(3)–C(9)–Rh(1)	113.2(2)	115.00(15)
N–C(carbene)–N		
N(1)–C(1)–N(2)	104.7(2)	104.91(19)
N(4)–C(9)–N(3)	104.2(3)	104.77(19)

Generation of Dicarbonyl Derivatives of bis-NHC Complexes. To estimate the ligand donor power, we looked at the ν_{CO} data from both the chelate and 2:1 bis-NHC complexes. As in the related rhodium NHC complexes,^{2b,c} the COD moieties in **3^{t-Bu}** and **4^{t-Bu}** were readily displaced by CO (1 atm, 15 min, CH₂Cl₂) so that the ν_{CO} of the dicarbonyl complexes could be measured (Table 3, see Discussion).

Discussion

Linker Dependence. In the *n*-Bu series, the reason that longer linkers ($n = 3, 4$) favor chelation was proposed to be their ability

(12) For other representative examples, see: (a) Quezada, C. A.; Garrison, J. C.; Tessier, C. A.; Youngs, W. J. *J. Organomet. Chem.* **2003**, *671*, 183–186. (b) Douthwaite, R. E.; Green, M. L. H.; Silcock, P. J.; Gomes, P. T. *Organometallics* **2001**, *20*, 2611–2615. (c) Bertrand, G.; Diez-Barra, E.; Fernandez-Baeza, J.; Gornitzka, H.; Moreno, A.; Otero, A.; Rodriguez-Curiel, R. I.; Tejada, J. *Eur. J. Inorg. Chem.* **1999**, 1965–1971. (d) Herrmann, W. A.; Elison, M.; Fischer, J.; Koecher, C.; Artus, G. R. J. *Angew. Chem., Int. Ed. Engl.* **1995**, *34*, 2371–2374.

(13) Baba, E.; Cundari, T. R.; Firkin, I. *Inorg. Chim. Acta* **2005**, *358*, 2867–2875.

Table 2. Variation of Yaw Distortion with Various Linkers and N-Substituents in Square Planar Bis-NHC Complexes

entry	M	linker (<i>n</i>)	wingtip	trans ligands	$\theta = (\alpha - \beta)/2$ (deg)	bite angle (deg)	M–NHC (Å)	ref
1	Rh(I)	1	<i>t</i> -Bu	COD	14	81.5	2.064	this report
2	Rh(I)	1	<i>t</i> -Bu	(CO) ₂	13	81.5	2.078	this report
3	Rh(I)	1	Me	COD	8	83.2	2.025	4b
4	Rh(I)	1	Me	(CO) ₂	7	83.5	2.062	4b
5	Rh(I)	2	<i>n</i> -Bu	COD	6	84.0	2.041	2b
6	Rh(I)	3	<i>n</i> -Bu	COD	3	87.6	2.034	2b
7	Rh(I)	4	<i>n</i> -Bu	(CO) ₂	1	91.1	2.082	2b
8	Rh(I)	1	Mesityl	COD	8	85.3	2.056	4a
9	Ni(II)	1	<i>t</i> -Bu	PMe ₃	10	84.9	1.941	5c
				Cl	15		1.872	
10	Ni(II)	1	<i>t</i> -Bu	bis-NHC	13	83.6	1.932	5c
11	Pd(II)	1	<i>t</i> -Bu	I ₂	14	83.4	2.004	5b
12	Pd(II)	1	Me	Br ₂	7	83.8	1.968	16
13	Pd(II)	1	Me	Cl ₂	6	83.8	1.957	17
14	Pd(II)	2	<i>t</i> -Bu	Me ₂	11	88.1	2.079	18
15	Ni(II)	2	<i>t</i> -Bu	Me ₂	12	88.9	1.909	12b
16	Ni(II)	2	<i>t</i> -Bu	PMe ₃	5	88.4	1.915	5c
				Cl	12		1.857	
17	Rh(I)	mono NHC ^a	<i>t</i> -Bu, Et	see note <i>a</i>	5	NA	2.031	19
18	Pd(II)	mono NHC ^b	<i>t</i> -Bu, py	see note <i>b</i>	9	NA	2.070	20
19	Ni(II)	mono NHC ^c	<i>t</i> -Bu, CMe ₂	see note <i>c</i>	15	NA	1.905	21b

^a [Rh(COD)(NHC)Cl], NHC = 1-ethyl-3-(*tert*-butyl)-4-ethylimidazolidin-2-ylidene. ^b [Pd(NHC)(C–P)(COOMe)], NHC = 1-(*tert*-butyl)-3-pyridylimidazol-2-ylidene, C–P = cyclometalated *o*-(di-*o*-tolylphosphino)CH₂C₆H₄. ^c [Ni(I'Bu)(η³-cyclooctenyl)], I'Bu = cyclometalated 1,3-di(*tert*-butyl)imidazol-2-ylidene.

Table 3. ν_{CO} of Bis-NHC Rh(I) Dicarbonyl Complexes^a

entry	type	linker length	wingtip	ν_{CO} (cm ⁻¹)	ν_{CO} average (cm ⁻¹)	Rh–CO ^b (Å)	diCO bite angle ^b (deg)	ref
1	2:1 ^c	2	<i>t</i> -Bu	1998, 2076	2037			this work
2	2:1	3	<i>t</i> -Bu	1994, 2072	2033			this work
3	2:1	4	<i>t</i> -Bu	1993, 2073	2033			this work
4	2:1	3	<i>n</i> -Bu	1996, 2076	2036			2b
5	2:1	4	<i>n</i> -Bu	1993, 2074	2034	1.90	94	2b
6	chelate ^d	1	<i>t</i> -Bu	2020, 2079	2050	1.90	92	this work
7	chelate	1	<i>n</i> -Bu	2017, 2076	2047			this work
8	chelate	1	Me	2019, 2077	2048	1.89	92	4b
9	chelate	2	<i>t</i> -Bu	2002, 2080	2041			this work
10	chelate	2	<i>n</i> -Bu	2015, 2077	2047			2b
11	bis-NHC ^e	NA	Me, Me	2018, 2078	2046			22

^a All measurements were made in CH₂Cl₂ except for entry 8 (KBr). ^b Where crystal structures are available. ^c Complex of type **3** where COD has been replaced by two carbonyl groups. ^d Complex analogous to **5**: [(chelate)Rh(CO)₂]PF₆. ^e [(NHC)₂Rh(CO)₂]OAc.

to avoid a steric clash between the *N*-substituents (R) and the other ligands (L) when the azole rings are nearly aligned along the $\pm z$ axis. However, in the current *t*-Bu series, steric interaction between the *N*-substituents (R··R) could become a significant counteracting factor disfavoring chelation, as the longer linkers would be expected to bring the two bulky R groups too close to each other. A steric clash between the *t*-Bu groups (Figures 3 and 4) could help explain the present observations that only the *n* = 1 and 2 cases can form chelates, while the *n* = 3 and 4 cases form 2:1 complexes. If so, examination of models suggested that for the trimethylene-linked case, at least, changing the *N*-substituent to *i*-Pr should relieve this proposed strain: the observed formation of the chelate product in the *i*-Pr case is consistent with this argument.

Effect of a Noncoordinating Anion. The anion also affects the choice between the two pathways. In order to form the cationic chelate complexes (e.g., **4aⁿ-Bu** or **4b^t-Bu**) instead of the 2:1 chloro complexes, the chloride has to leave the metal coordination sphere. This is expected to be favored if the Ag–NHC reagent does not already contain halide and therefore retains the ability to abstract the halide. An additional advantage of precipitating all the halide is the avoidance of the oxidative decomposition that tends to occur for **4a^t-Bu** in the presence of a halide ion, as discussed above. Since oxidative decomposition of the four-coordinate Rh(I) would be expected to go via a six-

coordinate Rh(III), the presence of a coordinating anion like the Br⁻ might well favor this process by ligation. A noncoordinating anion thus stabilizes the complex.

Structure of bis-NHC Chelates with *t*-Bu Wingtips. The structure of **4a^t-Bu** is highly distorted, with the COD moiety lying well out of the metal coordination plane as defined by C(carbene)–metal–C(carbene). The COD and the *t*-Bu substituents are distorted so as to put them on opposite sides of the metal coordination plane, as best seen in Figure 5.

Distortion of the Square Plane. At first glance, steric interactions between the COD and the *t*-Bu substituents appear to be the origin of the out-of-plane distortions observed in the structure of **4a^t-Bu**. However, a more detailed study of the structure showed no exceptionally close *t*-Bu–COD contacts (closest C··C: 3.51 Å). To test this point further, we expected the proposed R··L strain to be relieved if we replace the bulky COD with two COs. However, as shown in Figure 5, the structure of the dicarbonyl **5a^t-Bu** shows a distortion from planarity at the metal very similar to that seen for **4a^t-Bu** with the carbonyl carbon departing from the C(carbene)–Rh–C(carbene) plane by 0.35 Å. The observed distortion therefore cannot be attributed mainly to steric interactions between the COD and *t*-Bu. Agostic interactions between the Rh(I) center and the *t*-Bu C–H bonds in the out-of-plane direction would be weak, and the closest Rh··H distance, involving the

Table 4. Crystallographic Data for **4a^{t-Bu}** and **5a^{t-Bu}**

	4a^{t-Bu}	5a^{t-Bu}
empirical formula	C ₁₇ H ₂₄ F ₆ N ₄ O ₂ PRh	C ₂₃ H ₃₆ F ₆ N ₄ PRh
fw	564.28	616.44
λ (Å)	0.71073	0.71073
T (K)	123(2)	123(2)
cryst syst	monoclinic	monoclinic
space group	<i>P</i> 2(1)/ <i>c</i>	<i>P</i> 2(1)/ <i>c</i>
<i>a</i> (Å)	12.398(3)	24.919(5)
<i>b</i> (Å)	12.884(3)	13.643(3)
<i>c</i> (Å)	14.925(3)	15.498(3)
α (deg)	90	90
β (deg)	113.66(3)	92.83(3)
γ (deg)	90	90
<i>V</i> (Å ³)	2183.5(8)	5262.5(18)
<i>Z</i>	4	8
<i>D</i> _{calcd} (g cm ⁻³)	1.717	1.556
μ(Mo Kα) (cm ⁻¹)	9.27	7.71
cryst size (mm ³)	0.15 × 0.15 × 0.15	0.15 × 0.10 × 0.10
total, unique no. of reflns	8354, 5382	22 457, 12 908
<i>R</i> _{int}	0.0281	0.0345
no. of params, restrictions	280, 0	631, 0
final <i>R</i> indices [<i>I</i> > 2σ(<i>I</i>)] ^a	<i>R</i> : 0.0335, <i>R</i> _w : 0.0804	<i>R</i> : 0.0452, <i>R</i> _w : 0.1218
<i>R</i> indices (all data) ^a	<i>R</i> : 0.0456, <i>R</i> _w : 0.0849	<i>R</i> : 0.0666, <i>R</i> _w : 0.1320
goodness-of-fit on <i>F</i> ²	1.040	1.012
largest diff peak and hole (e ⁻ Å ⁻³)	0.512, -0.892	1.121, -0.925

$$^a R = \sum ||F_o| - |F_c|| / \sum |F_o|. R_w = \{ \sum [w(F_o^2 - F_c^2)^2] / \sum [w(F_o^2)^2] \}^{1/2}.$$

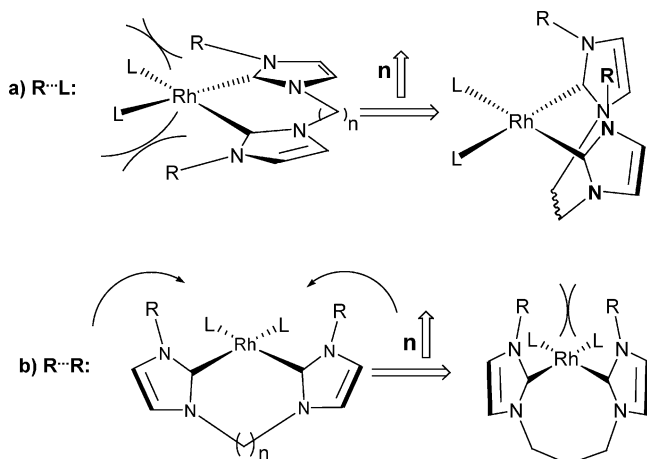


Figure 3. (a) Wingtip–ligand (R...L) interaction is relieved as *n* increases. (b) Wingtip–wingtip (R...R) interaction showing greater steric clash as *n* increases.

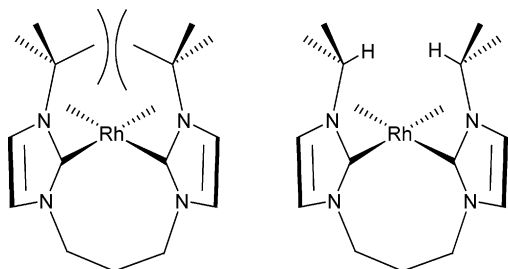


Figure 4. For a long linker (*n* = 3), changing from *t*-Bu to *i*-Pr is expected to relieve the R...R clash.

methylene linker (in **5a^{t-Bu}**: Rh–C: 3.06 Å; Rh–H: 2.86 Å), is not particularly short.¹⁴

Similar distortions have previously been attributed to the electronic preference for a non-square-planar structure in very electron-rich d⁸ complexes with π-accepting ligands, as previously observed for a Ru(0) species.¹⁵ By bending, the π-

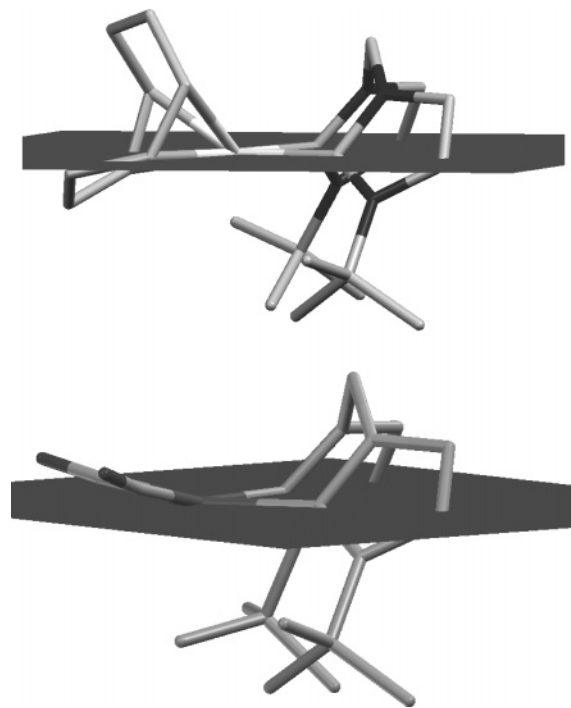


Figure 5. Out-of-plane distortion of **4a^{t-Bu}** (top) and of **5a^{t-Bu}** (bottom).

accepting CO ligand obtains some overlap of its π* with the high-energy d_{z²} orbital (Figure 6), enhancing back-donation from the electron-rich metal center. The COD system is expected to behave similarly.

In-Plane Distortion of the NHC. Another distortion (see Figure 7), which we term a yaw distortion, is probably the conformational strain imposed by the six-membered metallacycle, exacerbated by the additional steric interactions between the bulky *t*-Bu group and the metal center. We propose a simple descriptor of this in-plane distortion, $\theta = \frac{1}{2}(\alpha - \beta)$, which measures the difference in the two M–C–N angles.

(14) Crossley, I. R.; Hill, A. F.; Humphrey, E. R.; Smith, M. K. *Organometallics* **2006**, *25*, 2242–2247.

(15) Ogasawara, M.; Macgregor, S. A.; Streib, W. E.; Folting, K.; Eisenstein, O.; Caulton, K. G. *J. Am. Chem. Soc.* **1996**, *118*, 10189–10199.

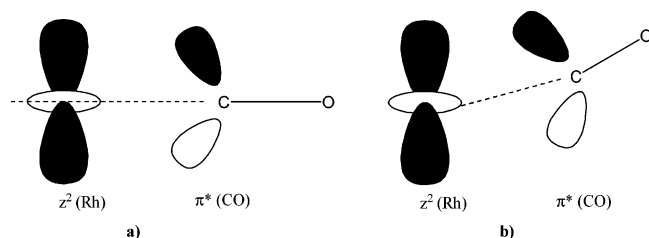


Figure 6. (a) In the undistorted case, no back-bonding from d_{z^2} is possible. (b) In the distorted case, back-donation from d_{z^2} becomes possible.¹⁵

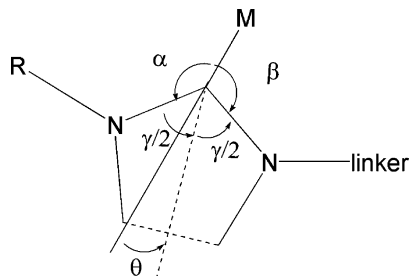


Figure 7. Extent of yaw distortion as defined by the angle $\theta = 1/2(\alpha - \beta)$.

This distortion of the M–NHC bond has not been discussed in detail before, so we have compared our data with some representative examples from the Cambridge Structural Database. The observed θ values, ranging up to 15° , are presented in Table 2. Also included are the bite angles (C–M–C) of the bis-NHCs and the sum of the angles at the carbene carbon ($\alpha + \beta + \gamma$). The latter remains within the range of $358\text{--}360^\circ$ (ideal = 360° for a planar system) for all surveyed structures, indicating that the metal remains in the azole plane and that the distortion of the metal–NHC bond occurs mainly in the NHC plane.

Origin of Yaw Distortion of M–NHC System. Ring Strain and θ . As can be seen in the series of Rh(I) complexes (Table 2), increasing metallacycle ring size causes a decrease in θ (entries 4–6), suggesting that ring strain is a contributing factor for the yaw distortion of the M–NHC. Going from a seven-membered ring (entry 5) to a nine-membered ring (entry 7), θ decreases from 6° to 1° . The most distorted M–NHC bonds are observed with five-membered metallacycles with *t*-Bu wingtips (e.g., entry 19).²¹

***N-t*-Bu-Induced Distortion.** As demonstrated in the structures of **4a^{t-Bu}** and **5a^{t-Bu}** (Table 2, entries 1 and 2) versus entries 3, 4, and 8, the yaw distortion is significantly increased by the presence of the *t*-Bu group. Similar effects can be seen for the Pd complexes in entries 11 versus 12. The *t*-Bu group has a bigger effect than the normally very bulky *N*-mesityl group

(entry 8), which shows no significant increase of θ over the very small *N*-methyl and *N*-*n*-butyl species. In the case of *t*-Bu, θ rises by at least 6° over the values found for the small Me and *n*-Bu groups. The mesityl group is probably capable of rotating about the C–N bond to minimize steric effects, something the *t*-Bu group cannot do. Monocarbene structures (entries 17, 18) suggest that the presence of a *t*-Bu group can alone be responsible for a yaw distortion with a θ up to 9° , but few examples of such complexes are yet known.

Effect of Non-NHC Ligand. A comparison of **4a^{t-Bu}** with its dicarbonyl analogue **5a^{t-Bu}** (Table 2, entries 1 and 2) shows that the influence of the two other ligands, COD or (CO)₂, on the yaw distortion of M–NHC is small. Entries 9 and 16 show an exceptional case, where the distortion seems to be predominantly the result of an electronic dissymmetry caused by having one PMe₃ and one Cl opposite the chelating NHC.

Estimation of Donor Power by ν_{CO} Measurements. As presented in Table 3, the ν_{CO} data for the 2:1 complexes are all near 2030 cm^{-1} and show no significant trend with wingtip substituent or linker. The chelate complexes show ν_{CO} values similar to those of the corresponding bis-NHC complex with two monodentate NHCs. Somewhat surprisingly, the highly distorted **5a^{t-Bu}** shows similar ν_{CO} values to the other chelate compounds. There is thus no clear evidence that the yaw distortion has a significant effect on the donor power of the chelate compounds.

Conclusion

We have synthesized a new series of bis-NHC rhodium(I) complexes, in which the bis-NHC coordinates either as a chelate or in a bridging 2:1 (metal:bis-NHC) fashion. Comparison with related studies suggests that the coordination mode is a result of the interplay between linker, *N*-substituent, and counterion effects. For the large *t*-Bu *N*-substituent, short linkers favor the chelate and long linkers favor the 2:1 complex, contrary to the prior findings with the small *n*-Bu substituent. In addition, the use of a noncoordinating anion favors chelate formation. Structural characterizations of two of the chelate complexes show a highly distorted structure with both an out-of-plane distortion and a “yaw” distortion of the metal–NHC group. A comparison of the data for related square planar bis-NHC structures suggests that the size of the yaw distortion is related to the size of the metallacycle ring as well as the size of the wingtip groups. On the basis of available ν_{CO} data, we find no evidence for any effect of the yaw distortion on the donor power of the NHC ligand.

Experimental Section

General Procedures. 1-(*tert*-Butyl)imidazole and 1-(isopropyl)imidazole were synthesized according to literature procedures²³ and purified by column chromatography (hexane/ethyl acetate/triethylamine). Disubstituted imidazolium salts **1a^{t-Bu}**, **1b^{t-Bu}**, and [Rh(COD)-Cl]₂²⁴ were prepared using standard literature methods. All other reagents and solvents were commercially available and used as received. Unless specified, all reactions were performed without precautions to exclude air or moisture. NMR spectroscopy was performed on Bruker spectrometers (500 or 400 MHz, ¹H NMR; 125 or 100 MHz, ¹³C NMR). Spectral assignments are based on

(22) Voutchkova, A. M.; Appelhans, L. N.; Chianese, A. R.; Crabtree, R. H. *J. Am. Chem. Soc.* **2005**, *127*, 17624–17625.

(23) (a) Liu, J. P.; Chen, J. B.; Zhao, J. F.; Zhao, Y. H.; Li, L.; Zhang, H. B. *Synthesis (Stuttgart)* **2003**, 2661–2666. (b) Gridnev, A. A.; Mihaltseva, I. M. *Synth. Commun.* **1994**, *24*, 1547–1555.

(24) Giordano, G.; Crabtree, R. H. *Inorg. Synth.* **1979**, *19*, 218–220.

(16) Herdtweck, E.; Muehlhofer, M.; Strassner, T. *Acta Crystallogr., Sect. E: Struct. Rep. Online* **2003**, *E59*, m970–m971.

(17) Strassner, T.; Muehlhofer, M.; Zeller, A.; Herdtweck, E.; Herrmann, W. A. *J. Organomet. Chem.* **2004**, *689*, 1418–1424.

(18) Douthwaite, R. E.; Green, M. L. H.; Silcock, P. J.; Gomes, P. T. *Dalton Trans.* **2002**, 1386–1390.

(19) Hahn, F. E.; Paas, M.; Le Van, D.; Lugger, T. *Angew. Chem., Int. Ed.* **2003**, *42*, 5243–5246.

(20) Frey, G. D.; Schutz, J.; Herdtweck, E.; Herrmann, W. A. *Organometallics* **2005**, *24*, 4416–4426.

(21) For some examples of single NHC as part of a metallacycle ring, see: (a) Scott, N. M.; Dorta, R.; Stevens, E. D.; Correa, A.; Cavallo, L.; Nolan, S. P. *J. Am. Chem. Soc.* **2005**, *127*, 3516–3526. (b) Caddick, S.; Cloke, F. G. N.; Hitchcock, P. B.; Lewis, A. K. D. *Angew. Chem., Int. Ed.* **2004**, *43*, 5824–5827. (c) Arnold, P. L.; Rodden, M.; Davis, K. M.; Scarisbrick, A. C.; Blake, A. J.; Wilson, C. *Chem. Commun.* **2004**, 1612–1613.

HMQC and COSY. Elemental analyses were performed by Atlantic Microlab, Inc. Water of crystallization was identified by ^1H NMR. Electrospray ionization mass spectra (ESI-MS) were recorded on a Micromass ZQ instrument using nitrogen as drying and nebulizing gas.

General Procedure for Synthesis of Bis(imidazolium) Salts.

The 1-alkylimidazole (4.2 mmol) and the corresponding dibromoalkane (2 mmol) were heated neat overnight in a sealed vial at 120 °C. The resulting solid was triturated with CH_2Cl_2 and washed with diethyl ether. The bis(imidazolium) salts were collected as white solids.

Trimethylenebis(*N*-(*tert*-butyl)imidazolium bromide) ($1\text{c}^t\text{-Bu}$).

From *N*-(*tert*-butyl)imidazole and 1,3-dibromopropane. Yield: 1.92 mmol, 99%. Anal. Calcd for $\text{C}_{17}\text{H}_{30}\text{Br}_2\text{N}_4\cdot\text{H}_2\text{O}$ (mol wt 468.27): C, 43.60; H, 6.89; N, 11.96. Found: C, 43.33; H, 7.11; N, 11.78. ^1H NMR (500 MHz, CDCl_3): δ 10.25 (s, 2H, NCHN); 8.20, 7.34 (s, 4H, CH(imid)); 4.71 (t, $^3J_{\text{H-H}} = 7.4$ Hz, 4H, NCH_2 (linker)), 2.97 (m, 2H, CH_2 linker), 1.69 (s, 18H, CH_3). $^{13}\text{C}\{^1\text{H}\}$ NMR (126 MHz, CDCl_3): δ 135.3, 124.0, 119.0 (C(imid)); 60.5 (CMe_3); 46.9, 31.3 (C(linker)); 30.1 (CH_3).

Tetramethylenebis(*N*-(*tert*-butyl)imidazolium bromide) ($1\text{d}^t\text{-Bu}$).

From *N*-(*tert*-butyl)imidazole and 1,4-dibromobutane. Yield: 1.97 mmol, 95%. Anal. Calcd for $\text{C}_{18}\text{H}_{32}\text{Br}_2\text{N}_4\cdot 2\text{H}_2\text{O}$ (mol wt 500.31): C, 43.21; H, 7.25; N, 11.20. Found: C, 42.92; H, 7.14; N, 11.08. ^1H NMR (500 MHz, CDCl_3): δ 10.42 (s, 2H, NCHN); 8.08, 7.31 (s, 4H, CH(imid)); 4.54 (t, $J_{\text{H-H}} = 6.5$ Hz, 4H, NCH_2), 2.24 (m, 4H, CH_2), 1.66 (s, 18H, CH_3). $^{13}\text{C}\{^1\text{H}\}$ NMR (126 MHz, CDCl_3): δ 135.5, 123.5, 118.8 (C(imid)); 60.4 (CMe_3); 48.8, 26.7 (C(linker)); 30.2 (CH_3).

Trimethylene Bis(*N*-(isopropyl)imidazolium bromide) ($1\text{c}^i\text{-Pr}$).

From *N*-(isopropyl)imidazole and 1,3-dibromopropane. Yield: 1.72 mmol, 90%. Anal. Calcd for $\text{C}_{15}\text{H}_{26}\text{Br}_2\text{N}_4\cdot\text{H}_2\text{O}$ (mol wt 440.22): C, 40.93; H, 6.41; N, 12.73. Found: C, 41.21; H, 6.47; N, 12.69. ^1H NMR (500 MHz, CDCl_3): δ 10.28 (s, 2H, NCHN); 8.21, 7.35 (s, 4H, CH(imid)); 4.69–4.75 (4+2H, NCH_2) and C(Me) $_2$ H(*i*-Pr), 2.92 (q, $^1J_{\text{H-H}} = 15$ Hz, 2H, CH_2), 1.61 (d, $^1J_{\text{H-H}} = 7.0$ Hz, 12H, CH_3). $^{13}\text{C}\{^1\text{H}\}$ NMR (126 MHz, CDCl_3): δ 135.5, 124.0, 119.6 (C(imid)); 53.4 (CHMe_2); 46.9, 31.0 (C(linker)); 23.1 (CH_3).

General Procedure for Synthesis of bis-NHC Rhodium Complexes by Transmetalation from Bromide Salts of Silver Carbenes. Bis(imidazolium) dibromide salts were dissolved in CH_2Cl_2 (25 mL) and vigorously stirred for 45 min with Ag_2O (4 equiv) at room temperature. The excess Ag_2O was removed by filtration and the solution heated to reflux temperature. Addition of $[\text{Rh}(\text{COD})\text{Cl}]_2$ (1 equiv) results in precipitation of the silver halide as a fine white powder, and the reaction was left to proceed to completion for another 30 min. The crude product mixture was filtered, and the filtrate was reduced in volume under reduced pressure and purified by column chromatography. Initial removal of unreacted $[\text{Rh}(\text{COD})\text{Cl}]_2$ by elution with CH_2Cl_2 was followed by elution with CH_2Cl_2 /acetone (50:50 v/v) to obtain the neutral 2:1 products. Cationic chelate products were eluted with an acetone solution of KPF_6 (10 mM). Excess KPF_6 in the resulting cationic products was removed by redissolving in CH_2Cl_2 and filtering through Celite. Removal of solvents yields the Rh complexes as yellow solids. The compounds can additionally be recrystallized from CH_2Cl_2 /ether or CH_2Cl_2 /pentane.

Ethylenebis(*N*-(*tert*-butyl)imidazol-2-ylidene)chloro(cyclooctadiene)rhodium} ($3\text{b}^t\text{-Bu}$). Ethylenebis(*N*-(*tert*-butyl)imidazolium bromide) used: 0.68 mmol. Yield: 0.46 mmol (68% based on Rh). Anal. Calcd for $\text{C}_{32}\text{H}_{50}\text{Cl}_2\text{N}_4\text{Rh}_2\cdot 2\text{H}_2\text{O}$ (mol wt 803.5): C, 47.83; H, 6.77; N, 6.97. Found: C, 47.88; H, 6.33; N, 6.80. ESI-MS (MeOH, 20 V, m/z): 731.8 ($\text{M}^+ - \text{Cl}$). ^1H NMR (500 MHz, CD_2Cl_2): δ 6.93 (d, $^3J_{\text{H-H}} = 1.8$ Hz, 2H, CH(imid)); 6.68 (d, $^3J_{\text{H-H}} = 1.8$ Hz, 2H, CH(imid)); 5.48 (m, 4H, CH_2 (linker)); 4.98 (m, 2H, CH(COD)); 4.86 (m, 2H, CH(COD)); 3.28 (m, 2H, CH(COD)); 3.22 (m, 2H, CH(COD)); 2.48–2.31 (m, 8H, CH(COD)); 1.91 (s,

18H, CH_3); 1.97–1.85 (m, 8H, CH_2 (COD)). $^{13}\text{C}\{^1\text{H}\}$ NMR (126 MHz, CD_2Cl_2): δ 179.9 (d, $^1J_{\text{C-Rh}} = 50.2$ Hz, C(carbene)), 123.4 (s, 2C, C(imid)), 118.9 (s, C(imid)), 97.1 (d, $^1J_{\text{C-Rh}} = 7.4$ Hz, CH(COD)), 94.5 (d, $^1J_{\text{C-Rh}} = 7.3$ Hz, 2C, CH(COD)), 71.0 (d, $^1J_{\text{C-Rh}} = 15.4$ Hz, CH(COD)), 69.2 (d, $^1J_{\text{C-Rh}} = 14.5$ Hz, CH(COD)); 58.8 (s, CMe_3); 52.3 (s, C(linker)); 33.4, 32.8, 29.7, 29.2 (s, CH_2 (COD)); 32.5 (s, CH_3).

Trimethylenebis(*N*-(*tert*-butyl)imidazol-2-ylidene)chloro(cyclooctadiene)rhodium} ($3\text{c}^t\text{-Bu}$).

Trimethylenebis(*N*-(*tert*-butyl)imidazolium bromide) used: 0.32 mmol. Yield: 0.15 mmol (47% based on Rh). Anal. Calcd for $\text{C}_{33}\text{H}_{52}\text{Cl}_2\text{N}_4\text{Rh}_2$ (mol wt 781.51): C, 50.72; H, 6.71; N, 7.17. Found: C, 50.90; H, 6.83; N, 7.26. ESI-MS (MeOH, 20 V, m/z): 745.7 ($\text{M}^+ - \text{Cl}$). ^1H NMR (400 MHz, CDCl_3 , a mixture of diastereomers, *dl:meso* (60:40), was present): δ 7.33 (d, $^3J_{\text{H-H}} = 1.9$ Hz, 2H, CH(imid)), 7.21 (d, $^3J_{\text{H-H}} = 1.9$ Hz, 1.3 H, CH(imid)), 7.02 (d, $^3J_{\text{H-H}} = 1.9$ Hz, 2H, CH(imid)), 6.79 (d, $^3J_{\text{H-H}} = 1.9$ Hz, 1.3 H, CH(imid)), 5.54 (m, 2H, CH(COD)), 5.53 (m, 1.3H, CH(COD)), 4.96–4.83 (m, 4+1.3H, NCH_2 (linker), CH(COD)), 4.77 (m, 2H, CH(COD)), 4.51 (m, 1.3H, CH(COD)), 4.29 (m, 2H, CH(COD)), 3.25–3.10 (m, 2.6+2+2H, NCH_2 (linker), CH(COD), CH_2 (linker)), 2.96 (m, 2H, CH_2 (linker)), 2.82 (m, 1.3H, CH(COD)), 2.49–2.01, 1.85–1.57 (m, 16+10.7H, CH_2 (COD)), 1.92 (s, 18H, CH_3), 1.88 (s, 12H, CH_3). $^{13}\text{C}\{^1\text{H}\}$ NMR (100 Hz, CDCl_3): δ 179.7 (d, $^1J_{\text{C-Rh}} = 50.8$ Hz, C(carbene)); 179.1 (d, $^1J_{\text{C-Rh}} = 50.2$ Hz, C(carbene)); 121.2, 120.9, 120.7, 120.4, 120.1, 119.9 (C(imid)); 96.4 (d, $^1J_{\text{C-Rh}} = 7.3$ Hz, CH(COD)), 95.8 (d, $^1J_{\text{C-Rh}} = 7.3$ Hz, CH(COD)), 94.6 (d, $^1J_{\text{C-Rh}} = 8.9$ Hz, CH(COD)), 94.2 (d, $^1J_{\text{C-Rh}} = 8.1$ Hz, CH(COD)); 71.0 (d, $^1J_{\text{C-Rh}} = 15.5$ Hz, CH(COD)), 70.2 (d, $^1J_{\text{C-Rh}} = 15.5$ Hz, CH(COD)); 57.6 (d, $^1J_{\text{C-Rh}} = 14.8$ Hz, CH(COD)), 55.7 (d, $^1J_{\text{C-Rh}} = 14.8$ Hz, CH(COD)); 58.4, 58.3 (s, CH_2 (linker)); 51.0, 50.4 (CMe_3); 34.0, 33.5, 33.0, 32.2, 31.5, 31.4, 30.1, 29.3, 29.0, 28.2 (s, CH_2 (COD), CH_2 (linker)); 32.6, 32.5 (s, CH_3).

Tetramethylenebis(*N*-(*tert*-butyl)imidazol-2-ylidene)chloro(cyclooctadiene)rhodium} ($3\text{d}^t\text{-Bu}$).

Tetramethylenebis(*N*-(*tert*-butyl)imidazolium bromide) used: 0.36 mmol. Yield: 0.18 mmol (50% based on Rh). Anal. Calcd for $\text{C}_{34}\text{H}_{54}\text{Cl}_2\text{N}_4\text{Rh}_2$ (mol wt 795.54): C, 51.33; H, 6.84; N, 7.04. Found: C, 51.11; H, 6.72; N, 6.84. ESI-MS (MeOH, 20 V, m/z): 759.79 ($\text{M}^+ - \text{Cl}$), 362.91 ($\text{M}^{2+} - 2\text{Cl}$). ^1H NMR (400 MHz, CD_2Cl_2 , *dl:meso*, 50:50): δ 7.05 (d, $^3J_{\text{H-H}} = 2.1$ Hz, 2H, CH(imid)); 7.00 (m, 4H, CH(imid)); 6.96 (d, $^3J_{\text{H-H}} = 2.1$ Hz, 2H, CH(imid)); 5.29, 4.79, 4.74, 4.49 (m, (8+8)H, CH(COD), NCH_2 (linker)); 3.24–3.11 (m, 8H, CH(COD)); 2.48–1.92, 1.83–1.65 (m, (32+8)H, CH_2 (COD), CH_2 (linker)); 1.86 (s, 18H, CH_3 (*t*-Bu)); 1.85 (s, 18H, CH_3 (*t*-Bu)). $^{13}\text{C}\{^1\text{H}\}$ NMR (100 Hz, CD_2Cl_2): δ 180.5 (d, $^1J_{\text{C-Rh}} = 50.3$ Hz, C(carbene)); 180.4 (d, $^1J_{\text{C-Rh}} = 49.8$ Hz, C(carbene)); 120.6, 120.5, 120.3, 120.2 (s, CH(imid)); 96.3, 94.0 (m, CH(COD)); 70.3, 67.9 (s, CH(COD)); 58.7, 52.8 (s, CH_2 (linker)); 33.6, 32.8, 32.6, 32.5, 32.2, 29.4, 29.2, 28.4 (m, CH_2 (linker), CMe_3 , CH_2 (COD), CH_3).

Trimethylenebis(*N*-(isopropyl)imidazol-2-ylidene)chloro(cyclooctadiene)rhodium} ($3\text{c}^i\text{-Pr}$).

The procedures were the same, except 0.5 equiv of $[\text{Rh}(\text{COD})\text{Cl}]_2$ was used. Trimethylenebis(*N*-(isopropyl)imidazolium bromide) used: 0.32 mmol. Yield: 0.14 mmol (44% based on Rh). Anal. Calcd for $\text{C}_{31}\text{H}_{48}\text{Cl}_2\text{N}_4\text{Rh}_2\cdot 1.5\text{H}_2\text{O}$ (mol wt 780.48): C, 47.71; H, 6.59; N, 7.18. Found: C, 47.72; H, 6.50; N, 7.18. ESI-MS (MeOH, 20 V, m/z): 745.7 ($\text{M}^+ - \text{Cl}$). ^1H NMR (500 MHz, CD_2Cl_2 , *dl:meso*, 60:40): δ 7.36 (d, $^3J_{\text{H-H}} = 2.0$ Hz, 2H, CH(imid)), 7.29 (d, $^3J_{\text{H-H}} = 2.0$ Hz, 1.3H, CH(imid)), 6.95 (d, $^3J_{\text{H-H}} = 2.0$ Hz, 2H, CH(imid)), 6.65 (d, $^3J_{\text{H-H}} = 2.0$ Hz, 1.3H, CH(imid)), 5.80–5.70 (m, 2+1.3H, NCH_2 (linker)), 5.01–4.85 (m, 2+1.3+4+2.6H, NCH_2 (linker), CH(COD)); 4.32 (m, 1.3H, CMe_2H); 4.16 (m, 2H, CMe_2H); 3.31–3.20 (m, 4+2.6H, CH(COD)); 2.49–2.27 (m, 8+5.2H, CH_2 (COD)); 2.09–1.87 (m, 8+5.2H, CH_2 (COD)), 1.51 (d, $^1J_{\text{H-H}} = 6.7$ Hz, 6H, CH_3); 1.49–1.46 (m, 6+3.9H, CH_3); 1.41 (d, $^1J_{\text{H-H}} = 6.7$ Hz, 3.9H, CH_3). $^{13}\text{C}\{^1\text{H}\}$ NMR (126 MHz): δ 181.3 (d, $^1J_{\text{Rh-C}} = 51.4$ Hz, C(carbene)); 180.0 (d, $^1J_{\text{Rh-C}} = 51.0$

Hz, C(carbene)); 122.5 (s, C(imid)); 122.3 (s, C(imid)); 117.0 (s, C(imid)); 116.6 (s, C(imid)); 98.5 (d, $^1J_{\text{Rh-C}} = 6.7$ Hz, CH(COD)); 97.9, 97.8 (m, CH(COD)); 69.1, 68.8, 68.4, 69.1 (m, CH(COD)); 53.2, 53.1 (s, CH₂(linker)), 49.7, 48.8 (s, CHMe₂); 33.9, 33.4, 33.0, 32.0, 31.1 (s, CH₂(COD), CH₂(linker)); 30.0, 29.5, 29.3, 28.9 (s, CH₂(COD)); 24.4, 24.2, 23.5, 23.3 (s, CH₃).

Trimethylenebis(*N*-(isopropyl)imidazol-2-ylidene)(cyclooctadiene)rhodium Hexafluorophosphate (4c^{i-Pr}). After elution of 3c^{i-Pr} by CH₂Cl₂/acetone (50:50) from the column in the above procedure, 4c^{i-Pr} was obtained by further elution with acetone/KPF₆ (150 mg). Yield: 0.08 mmol (13% based on Rh). Anal. Calcd for C₂₃H₃₆F₆N₄PRh·0.5H₂O (mol wt 625.44): C, 44.17; H, 5.96; N, 8.96. Found: C, 44.15; H, 5.84; N, 8.87. ESI-MS (MeOH, 20 V, *m/z*): 471.7 (M⁺). ¹H NMR (400 MHz, CD₂Cl₂): δ 6.89, 6.79 (d, $^3J_{\text{H-H}} = 2.0$ Hz, 4H, CH(imid)); 5.00 (hep, $^3J_{\text{H-H}} = 6.9$ Hz, 2H, NCHMe₂); 4.90, 4.23 (m, 4H, CH₂(linker)); 2.37, 2.15 (m, 4+1+4H, CH₂(linker), CH₂(COD)); 1.34 (d, $^3J_{\text{H-H}} = 6.9$ Hz) 12H, CH₃. ¹³C{¹H}NMR (100 MHz): δ 180.9 (d, $^1J_{\text{Rh-C}} = 54.4$ Hz, C(carbene)); 124.1, 117.3 (s, C(imid)); 90.4 (d, $^1J_{\text{Rh-C}} = 8.3$ Hz, C(COD)); 88.6 (d, $^1J_{\text{Rh-C}} = 7.3$ Hz, C(COD)); 53.6 (s, CHMe₂); 53.2 (s, NCH₂(linker)); 33.4 (s, CH₂(linker)); 31.3, 31.0 (s, CH₂(COD)); 25.8, 24.1 (s, CH₃).

General Procedure for Synthesis of Bis-NHC Rhodium Complexes by Transmetalation from Hexafluorophosphate Salts of Silver Carbenes. Bis(imidazolium) dibromide/diiodide salts (0.5 mmol) and Ag₂O (4 equiv) were stirred vigorously in water at 0 °C for 30 min. The solution was filtered through Celite to remove excess Ag₂O, and a saturated aqueous KPF₆ (2.5 equiv) was added. The resultant white precipitate was dried under vacuum and dissolved in refluxing CH₂Cl₂. Addition of [Rh(COD)Cl]₂ (0.5 equiv) resulted in precipitation of silver halide as a fine white powder, and the reaction was left to proceed in CH₂Cl₂ for another 30 min. The crude product mixture was filtered, reduced in volume under reduced pressure, and purified by column chromatography as above. Elution by acetone/KPF₆ yields the cationic chelate compounds as yellow solids. The compounds can be further recrystallized from dichloromethane/pentane.

[Methylenebis(*N*-(*tert*-butyl)imidazol-2-ylidene)](cyclooctadiene)rhodium Hexafluorophosphate (4a^{t-Bu}). Yield: 0.07 mmol (29% based on Rh). Anal. Calcd for C₂₃H₃₆F₆N₄PRh (mol wt 616.43): C, 44.81; H, 5.89; N, 9.09. Found: C, 44.61; H, 5.99; N, 9.02. ESI-MS (MeOH, 20 V, *m/z*): 471.7 (M⁺), 363.7 (M⁺ - COD). ¹H NMR (400 MHz, CD₂Cl₂): δ 7.32, 6.92 (d, $^3J_{\text{H-H}} = 2.2$ Hz, 4H, CH(imid)); 6.86, 6.07 (AB system, $^2J_{\text{H-H}} = 12.7$ Hz, 2H, CH₂(linker)); 4.50, 4.43 (m, 4H, CH(COD)); 2.42–1.96 (m, 8H, CH₂(COD)); 1.57 (s, 18H, CH₃). ¹³C{¹H} NMR (125 Hz, CD₂Cl₂): δ 180.4 (d, $^1J_{\text{Rh-C}} = 51.8$ Hz, C(carbene)); 121.9, 119.2 (s, CH(imid)); 90.5 (d, $^1J_{\text{Rh-C}} = 9.5$ Hz, CH(COD)); 85.2 (d, $^1J_{\text{Rh-C}} = 7.4$ Hz, CH(COD)); 65.5 (s, CH₂(linker)); 58.4 (s, CMe₃); 32.2 (s, CH₃); 30.9 (s, CH₂(COD)).

[Methylenebis(*N*-*n*-butylimidazol-2-ylidene)](cyclooctadiene)rhodium Hexafluorophosphate (4a^{n-Bu}). The procedure is analogous to the above except that the transmetalation reaction was carried out using standard Schlenk techniques in degassed CH₂Cl₂, and the resulting orange compound was obtained by removal of solvents under reduced pressure. Yield: 0.07 mmol (31% based

on Rh). Elemental analysis was not possible in this case because of the instability of the compound. ESI-MS (MeOH, 20 V, *m/z*): 363.6 (M⁺ - COD). ¹H NMR: δ 7.32 (d, $^1J_{\text{H-H}} = 2.0$ Hz, 2H, CH(imid)); 5.82 (d, $^1J_{\text{H-H}} = 2.0$ Hz, 2H, CH(imid)); 6.43, 6.00 (AB system, $^2J_{\text{H-H}} = 13.0$ Hz, 2H, CH₂(linker)); 4.80–4.72 (m, 4H, CH(COD)); 3.91 (m, 4H, NCH₂(*n*Bu)); 2.50–2.09 (m, 8H, CH₂(COD)); 1.86–1.57 (m, 4H, CH₂(*n*Bu)); 1.31–1.23 (m, 4H, CH₂(*n*Bu)); 0.94 (t, $^3J_{\text{H-H}} = 7.9$ Hz, 6H, CH₃). ¹³C{¹H} NMR (125 Hz, CD₂Cl₂): δ 180.9 (d, $^1J_{\text{C-Rh}} = 53.3$ Hz, C(carbene)); 121.8, 121.3 (s, C(imid)); 92.3 (d, $^1J_{\text{C-Rh}} = 8.6$ Hz, CH(COD)), 87.0 (d, $^1J_{\text{C-Rh}} = 7.5$ Hz, CH(COD)); 53.6 (s, CH₂(linker)); 50.7 (s, NCH₂(*n*Bu)); 34.3 (s, CH₂(*n*Bu)); 31.2, 31.0 (s, CH₂(COD)); 20.3 (s, CH₂(*n*Bu)); 14.0 (s, CH₃).

[Methylenebis(*N*-(*tert*-butyl)imidazol-2-ylidene)](dicarbonyl)rhodium Hexafluorophosphate (5a^{t-Bu}). CO (1 atm) was passed through a concentrated solution of 4a^{t-Bu} for 20 min. The resulting solution was reduced in volume under reduced pressure, and 5a^{t-Bu} was recrystallized from CH₂Cl₂/pentane as yellow crystals. Anal. Calcd for C₁₇H₂₄F₆N₄O₂PRh (mol wt 564.27): C, 36.19; H, 4.29; N, 9.93. Found: C, 36.19; H, 4.30; N, 9.90. ESI-MS (MeOH, 20 V, *m/z*): 419.6 (M⁺). IR (cm⁻¹): 2020, 2079. ¹H NMR: δ 7.47, 7.11 (d, $^1J_{\text{H-H}} = 2$ Hz, 4H, CH(imid)); 6.25, 6.09 (AB system, $^2J_{\text{H-H}} = 13.1$ Hz, 2H, NCH₂(linker)); 1.63 (s, 18H, CH₃). ¹³C{¹H} NMR (125 MHz, CDCl₃): δ 187.5 (d, $^1J_{\text{C-Rh}} = 59.3$ Hz, CO); 171.4 (d, $^1J_{\text{C-Rh}} = 49.4$ Hz, C(carbene)); 122.7, 120.1 (s, CH(imid)); 65.1 (s, NCH₂(linker)); 59.4 (s, CMe₃); 31.8 (s, CH₃).

X-ray Crystallography. Crystals suitable for X-ray diffraction studies were obtained by slow diffusion of pentane into concentrated CH₂Cl₂ solutions of the complexes 4a^{t-Bu} and 5a^{t-Bu}. Data were collected on a Nonius KappaCCD diffractometer with graphite-monochromated Mo Kα radiation and processed and scaled using the DENZO software package.²⁵ The structure was solved by direct methods and expanded using Fourier techniques.²⁶ The non-hydrogen atoms were refined anisotropically, and hydrogen atoms were treated as idealized contributions.

Survey of Crystal Structures. Structural search in the Cambridge Structural Database (CSD) was performed using the ConQuest software.²⁷ Bond length and bond angle measurements were made by the built-in functions.

Acknowledgment. We thank the U.S. DOE and the Johnson Matthey Co. for support. We also gratefully acknowledge Prof. Eduardo Peris (Jaume I University, Spain) for helpful discussions and Leah Appelhans and Macarena Poyatos for assistance.

Supporting Information Available: Spectral evidence for 4b^{t-Bu}, an extended version of Table 2, as well as further crystallographic data including the CIF files of 4a^{t-Bu} and 5a^{t-Bu} are available on the Internet at <http://pubs.acs.org>.

OM0607189

(25) Otwinowski, Z.; Minor, W. In *Methods in Enzymology*; Vol. 276: Macromolecular Crystallography, part A; Carter, C. W. J., Sweet, R. M., Eds.; Academic Press: New York, 1997; pp 307–326.

(26) Sheldrick G. M. *Acta Crystallogr.* **1990**, *A46*, 467–473.

(27) Bruno, I. J.; Cole, J. C.; Edgington, P. R.; Kessler, M.; Macrae, C. F.; McCabe, P.; Pearson, J.; Taylor, R. *Acta Crystallogr.* **2002**, *B58*, 389–397.